

Scattering from an Arbitrarily Incident Plane Wave by a PEMC Elliptic Cylinder Confocally Coated with a Chiral Material

A-K. Hamid

Department of Electrical and Computer Engineering
University of Sharjah, P. O. Box 27272, Sharjah, United Arab Emirates
akhamid@sharjah.ac.ae

Abstract — An analytic solution to the problem of scattering of a plane electromagnetic wave by a chirally coated elliptic cylinder defined by PEMC boundary condition has been obtained by expanding the different electromagnetic fields in terms of appropriate elliptic wave functions and a set of expansion coefficients. The expansion coefficients associated with the transmitted field inside the coating as well as the scattered field outside the coating are unknown and will be obtained by applying the boundary conditions at various layers. Numerical results have been presented graphically to show the effects of chiral and PEMC materials simultaneously on the bistatic width of scattering from coated elliptic cylinder.

Index Terms — Bistatic, chiral, elliptic cylinder, Mathieu functions, PEMC.

I. INTRODUCTION

Since the introduction of PEMC materials in 2005 [1], there has been a lot of research into scattering from different types of both two- and three-dimensional PEMC objects [2-12]. This has recently led to an interest on research involving coated PEMC objects [13-14]. As described in [1], a PEMC medium is a generalized form of a perfect electric conducting (PEC) and a perfect magnetic conducting (PMC) medium in which certain linear combinations of electromagnetic fields become extinct [15], and is definable by a single real-valued parameter known as the PEMC admittance. A null admittance corresponds to a PMC medium and an admittance of infinity corresponds to a PEC medium, when the field magnitudes are finite [16]. A PEMC material acts as a perfect reflector of electromagnetic waves, but differs from PEC and PMC materials due to the fact that it produces a reflected wave with a cross-polarized field component [17-22].

The elliptic cylinder is a geometry that has been extensively analyzed in the literature due to its ability to produce cylinders of different cross sectional shapes, by

changing the axial ratio of the ellipse. Moreover, since the elliptic cylindrical coordinate system is one of the coordinate systems in which the wave equation is separable, solutions to problems involving elliptic cylinders can be obtained in closed form.

In this paper, we present the analysis corresponding to the scattering from a chiral coated PEMC elliptic cylinder of arbitrary axial ratio, when it is excited by either a plane wave of arbitrary polarization and angle of incidence. Such solution is valuable, since it can be used for validating solutions obtained using other methods. The analysis and the software used for obtaining the results have been validated by calculating the normalized scattering widths for a PEMC coated elliptic [22] when it is illuminated by a plane wave. It was shown graphically that these results are in very good agreement with the corresponding results obtained using various values of admittances for coated PEMC elliptic cylinder.

II. FORMULATION

Consider a linearly polarized uniform plane electromagnetic wave arbitrarily incident on an infinitely long PEMC elliptic cylinder confocally coated with a chiral material. The semi-major and semi-minor axis lengths of the uncoated cylinder are denoted by a_0 and b_0 , and those of the coated cylinder are denoted by a_c and b_c , respectively. The coated cylinder is assumed to be located in free space, with the incident wave making an angle φ_i with the negative x-axis of a Cartesian coordinate system as shown in Fig. 1. It is beneficial to define the x and y coordinates of the Cartesian coordinate system in terms u, v, z of an elliptical coordinate system where $x = F \cosh u \cos v$, $y = F \sinh u \sin v$, with F being the semi-focal length of the ellipse. A time dependence of $\exp(j\omega t)$ with ω being the angular frequency, is assumed throughout the analysis, but suppressed for convenience. The analysis is conducted for an incident uniform plane wave of transverse magnetic (TM) polarization. The analysis corresponding to a plane wave

of transverse electric (TE) polarization can be obtained from that for a plane wave of TM polarization, using duality.

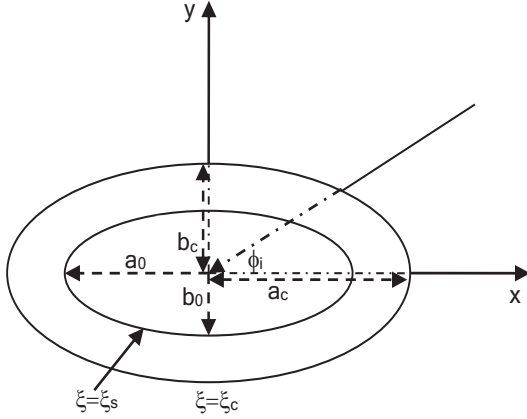


Fig. 1. Geometry of the chiral coated PEMC elliptic cylinder.

Considering a TM polarized arbitrarily incident plane wave of unit amplitude, we can expand the incident electric field component as [23]:

$$E_z^{inc} = \sum_{q,n} A_{qn} R_{qn}^{(1)}(c, \xi) S_{qn}(c, \eta), \quad (1)$$

where $R_{qn}^{(i)}(c, \xi)$ and $S_{qn}(c, \eta)$ are the i -th order of the radial and angular Mathieu functions respectively, where $q = e, o$ stands for even and odd solution, and

$$A_{qn} = j^n \frac{\sqrt{8\pi}}{N_{qn}(c)} S_{qn}(c, \cos \phi_i), \quad (2)$$

in which $c = kF$ with k being the wavenumber of the medium outside the cylinder and $N_{qn}(c)$ is the normalization constant associated with $S_{qn}(c, \eta)$. Using Maxwell's equations we can expand the incident magnetic field component as:

$$H_v^{inc} = \frac{1}{jkZh} \sum_{q,n} A_{qn} R_{qn}^{(1)'}(c, \xi) S_{qn}(c, \eta), \quad (3)$$

where $h = F\sqrt{\cosh^2 u - \cos^2 v}$, with $\xi = \cosh u$, $\eta = \cos v$, Z is the wave impedance of the medium outside the cylinder, and the prime denoting the differentiation with respect to u .

Since the cylinder comprises of a PEMC material, the scattered field consists of both co- and cross-polar components. These can be expanded as:

$$E_z^s = \sum_{q,n} B_{qn} R_{qn}^{(4)}(c, \xi) S_{qn}(c, \eta), \quad (4)$$

$$E_v^s = -\frac{1}{kh} \sum_{q,n} C_{qn} R_{qn}^{(4)'}(c, \xi) S_{qn}(c, \eta), \quad (5)$$

$$H_z^s = \frac{j}{Z} \sum_{q,n} C_{qn} R_{qn}^{(4)}(c, \xi) S_{qn}(c, \eta), \quad (6)$$

$$H_v^s = \frac{1}{jkZh} \sum_{q,n} B_{qn} R_{qn}^{(4)'}(c, \xi) S_{qn}(c, \eta), \quad (7)$$

in which C_{qn} and B_{qn} are the unknown co- and cross-scattered field expansion coefficients.

The fields within the chiral coating also have both co- and cross-polar components, comprising of left- and right-handed parts. These can be expanded as:

$$E_z^c = \sum_{q,n} \{ [D_{qn} R_{qn}^{(1)}(c_R, \xi) + P_{qn} R_{qn}^{(2)}(c_R, \xi)] S_{qn}(c_R, \eta) + [F_{qn} R_{qn}^{(1)}(c_L, \xi) + Q_{qn} R_{qn}^{(2)}(c_L, \xi)] S_{qn}(c_L, \eta) \}, \quad (8)$$

$$E_v^c = \sum_{q,n} \left\{ -\frac{1}{k_R h} [D_{qn} R_{qn}^{(1)'}(c_R, \xi) + P_{qn} R_{qn}^{(2)'}(c_R, \xi)] S_{qn}(c_R, \eta) + \frac{1}{k_L h} [F_{qn} R_{qn}^{(1)'}(c_L, \xi) + Q_{qn} R_{qn}^{(2)'}(c_L, \xi)] S_{qn}(c_L, \eta) \right\}, \quad (9)$$

$$H_z^c = \frac{j}{Z_c} \sum_{q,n} \{ [D_{qn} R_{qn}^{(1)}(c_R, \xi) + P_{qn} R_{qn}^{(2)}(c_R, \xi)] S_{qn}(c_R, \eta) - [F_{qn} R_{qn}^{(1)}(c_L, \xi) + Q_{qn} R_{qn}^{(2)}(c_L, \xi)] S_{qn}(c_L, \eta) \}, \quad (10)$$

$$H_v^c = \frac{j}{Z_c} \sum_{q,n} \left\{ -\frac{1}{k_R h} [D_{qn} R_{qn}^{(1)'}(c_R, \xi) + P_{qn} R_{qn}^{(2)'}(c_R, \xi)] S_{qn}(c_R, \eta) - \frac{1}{k_L h} [F_{qn} R_{qn}^{(1)'}(c_L, \xi) + Q_{qn} R_{qn}^{(2)'}(c_L, \xi)] S_{qn}(c_L, \eta) \right\}, \quad (11)$$

where $D_{qn}, F_{qn}, P_{qn}, Q_{qn}$ are the unknown field expansion coefficients, $c_R = k_R F$, $c_L = k_L F$, with the wavenumbers k_R and k_L corresponding to the right- and left-handed waves inside the chiral medium given by $k_{R,L} = \omega \sqrt{\mu \varepsilon_c} \pm \omega \mu \zeta_c$, in which ζ_c is the chirality admittance and ε_c is the effective permittivity defined by $\varepsilon_c = \mu + \varepsilon \zeta_c^2$ with ε and μ being the permittivity and permeability of the chiral medium, and Z_c is the wave impedance in the chiral medium, given by $Z_c = \sqrt{\mu / \varepsilon_c}$.

The boundary conditions at the surface $\xi = \xi_c$ of the coating require the continuity of the tangential components of the electric and magnetic fields across the boundary. These can be written mathematically as:

$$E_z^c = E_z^i + E_z^s, \quad (12)$$

$$E_v^c = E_v^i + E_v^s, \quad (13)$$

$$H_z^c = H_z^i + H_z^s, \quad (14)$$

$$H_v^c = H_v^i + H_v^s. \quad (15)$$

Similarly, the boundary conditions at the surface $\xi = \xi_s$ of the PEMC elliptic cylinder can be written using the PEMC admittance M as:

$$H_z^c + ME_z^c = 0, \quad (16)$$

$$H_v^c + ME_v^c = 0. \quad (17)$$

Substituting for the electric field components in (12)-(13) in terms of their respective expansions, we get:

$$\begin{aligned} & \sum_{q,n} \{ [D_{qn} R_{qn}^{(1)}(c_R, \xi_c) + P_{qn} R_{qn}^{(2)}(c_R, \xi_c)] S_{qn}(c_R, \eta) \\ & + [F_{qn} R_{qn}^{(1)}(c_L, \xi_c) + Q_{qn} R_{qn}^{(2)}(c_L, \xi_c)] S_{qn}(c_L, \eta) \} \quad (18) \\ & = \sum_{q,n} [A_{qn} R_{qn}^{(1)}(c, \xi_c) + B_{qn} R_{qn}^{(4)}(c, \xi_c)] S_{qn}(c, \eta), \end{aligned}$$

$$\begin{aligned} & \sum_{q,n} \left\{ -\frac{1}{k_R h} [D_{qn} R_{qn}^{(1)'}(c_R, \xi_c) + P_{qn} R_{qn}^{(2)'}(c_R, \xi_c)] S_{qn}(c_R, \eta) \right. \\ & \left. + \frac{1}{k_L h} [F_{qn} R_{qn}^{(1)'}(c_L, \xi_c) + Q_{qn} R_{qn}^{(2)'}(c_L, \xi_c)] S_{qn}(c_L, \eta) \right\} \quad (19) \\ & = -\frac{1}{kh} \sum_{q,n} C_{qn} R_{qn}^{(4)'}(c, \xi_c) S_{qn}(c, \eta). \end{aligned}$$

Substituting for the magnetic field components in (14)-(15) in terms of their respective expansions yields:

$$\begin{aligned} & \frac{j}{Z_c} \sum_{q,n} \{ [D_{qn} R_{qn}^{(1)}(c_R, \xi_c) + P_{qn} R_{qn}^{(2)}(c_R, \xi_c)] S_{qn}(c_R, \eta) \\ & - [F_{qn} R_{qn}^{(1)}(c_L, \xi_c) + Q_{qn} R_{qn}^{(2)}(c_L, \xi_c)] S_{qn}(c_L, \eta) \} \quad (20) \\ & = \frac{j}{Z} \sum_{q,n} C_{qn} R_{qn}^{(4)}(c, \xi_c) S_{qn}(c, \eta), \end{aligned}$$

$$\begin{aligned} & \sum_{q,n} \left\{ \frac{1}{jk_R h Z_c} [D_{qn} R_{qn}^{(1)'}(c_R, \xi_c) + P_{qn} R_{qn}^{(2)'}(c_R, \xi_c)] S_{qn}(c_R, \eta) \right. \\ & \left. + \frac{1}{jk_L h Z_c} [F_{qn} R_{qn}^{(1)'}(c_L, \xi_c) + Q_{qn} R_{qn}^{(2)'}(c_L, \xi_c)] S_{qn}(c_L, \eta) \right\} \quad (21) \\ & = \sum_{q,n} \frac{1}{jkhZ} [A_{qn} R_{qn}^{(1)'}(c, \xi_c) + B_{qn} R_{qn}^{(4)'}(c, \xi_c)] S_{qn}(c, \eta). \end{aligned}$$

Substituting for the field components in (17) and (18) in terms of their expansions, we get:

$$\begin{aligned} & \frac{j}{Z_c} \sum_{q,n} \{ [D_{qn} R_{qn}^{(1)}(c_R, \xi_s) + P_{qn} R_{qn}^{(2)}(c_R, \xi_s)] S_{qn}(c_R, \eta) \\ & - [F_{qn} R_{qn}^{(1)}(c_L, \xi_s) + Q_{qn} R_{qn}^{(2)}(c_L, \xi_s)] S_{qn}(c_L, \eta) \} \quad (22) \\ & + M \sum_{q,n} [D_{qn} R_{qn}^{(1)}(c_R, \xi_s) + P_{qn} R_{qn}^{(2)}(c_R, \xi_s)] S_{qn}(c_R, \eta) \\ & + [F_{qn} R_{qn}^{(1)}(c_L, \xi_s) + Q_{qn} R_{qn}^{(2)}(c_L, \xi_s)] S_{qn}(c_L, \eta) = 0, \end{aligned}$$

$$\begin{aligned} & \sum_{q,n} \left\{ \frac{1}{jk_R h Z_c} [D_{qn} R_{qn}^{(1)'}(c_R, \xi_s) + P_{qn} R_{qn}^{(2)'}(c_R, \xi_s)] S_{qn}(c_R, \eta) \right. \\ & \left. + \frac{1}{jk_L h Z_c} [F_{qn} R_{qn}^{(1)'}(c_L, \xi_s) + Q_{qn} R_{qn}^{(2)'}(c_L, \xi_s)] S_{qn}(c_L, \eta) \right\} \quad (23) \\ & + M \sum_{q,n} -\frac{1}{k_R h} [D_{qn} R_{qn}^{(1)'}(c_R, \xi_s) + P_{qn} R_{qn}^{(2)'}(c_R, \xi_s)] S_{qn}(c_R, \eta) \\ & + \frac{1}{k_L h} [F_{qn} R_{qn}^{(1)'}(c_L, \xi_s) + Q_{qn} R_{qn}^{(2)'}(c_L, \xi_s)] S_{qn}(c_L, \eta) = 0. \end{aligned}$$

If both sides of equations (18)-(23) are multiplied by $S_{qn}(c, \eta)$ and integrated over η from -1 to 1, then considering the orthogonality of the angular Mathieu functions, we can write these equations after a rearrangement as:

$$\begin{aligned} & [D_{qn} R_{qn}^{(1)}(c_R, \xi_c) + P_{qn} R_{qn}^{(2)}(c_R, \xi_c)] M_{qn}^R(c_R, c) \\ & + [F_{qn} R_{qn}^{(1)}(c_L, \xi_c) + Q_{qn} R_{qn}^{(2)}(c_L, \xi_c)] M_{qn}^L(c_L, c) = \quad (24) \\ & [A_{qn} R_{qn}^{(1)}(c, \xi_c) + B_{qn} R_{qn}^{(4)}(c, \xi_c)] N_{qn}(c), \end{aligned}$$

$$\begin{aligned} & \frac{k}{k_R} [D_{qn} R_{qn}^{(1)'}(c_R, \xi_c) + P_{qn} R_{qn}^{(2)'}(c_R, \xi_c)] M_{qn}^R(c_R, c) \\ & - \frac{k}{k_L} [F_{qn} R_{qn}^{(1)'}(c_L, \xi_c) + Q_{qn} R_{qn}^{(2)'}(c_L, \xi_c)] M_{qn}^L(c_L, \eta) = \quad (25) \\ & C_{qn} R_{qn}^{(4)'}(c, \xi_c) N_{qn}(c), \end{aligned}$$

$$\begin{aligned} & D_{qn} R_{qn}^{(1)}(c_R, \xi_c) + P_{qn} R_{qn}^{(2)}(c_R, \xi_c) M_{qn}^R(c_R, c) \\ & - [F_{qn} R_{qn}^{(1)}(c_L, \xi_c) + Q_{qn} R_{qn}^{(2)}(c_L, \xi_c)] M_{qn}^L(c_L, c) = \quad (26) \\ & \frac{Z_c}{Z} C_{qn} R_{qn}^{(4)}(c, \xi_c) N_{qn}(c), \end{aligned}$$

$$\begin{aligned} & \left(\frac{kZ}{k_R Z_c} \right) [R_{qn}^{(1)'}(c_R, \xi_c) + P_{qn} R_{qn}^{(2)'}(c_R, \xi_c)] M_{qn}^R(c_R, c) \\ & + \left(\frac{kZ}{k_L Z_c} \right) [F_{qn} R_{qn}^{(1)'}(c_L, \xi_c) + Q_{qn} R_{qn}^{(2)'}(c_L, \xi_c)] M_{qn}^L(c_L, c) \quad (27) \\ & = [A_{qn} R_{qn}^{(1)'}(c, \xi_c) + B_{qn} R_{qn}^{(4)'}(c, \xi_c)] N_{qn}(c), \end{aligned}$$

$$\begin{aligned} & (1 - jMZ_c) [D_{qn} R_{qn}^{(1)}(c_R, \xi_s) + P_{qn} R_{qn}^{(2)}(c_R, \xi_s)] M_{qn}^R(c_R, c) \\ & - (1 + jMZ_c) [F_{qn} R_{qn}^{(1)}(c_L, \xi_s) + Q_{qn} R_{qn}^{(2)}(c_L, \xi_s)] M_{qn}^L(c_L, c) = 0, \quad (28) \end{aligned}$$

$$\begin{aligned} & (1 - jMZ_c) \left(\frac{k}{k_R} \right) [D_{qn} R_{qn}^{(1)'}(c_R, \xi_s) + P_{qn} R_{qn}^{(2)'}(c_R, \xi_s)] M_{qn}^R(c_R, c) \\ & + (1 + jMZ_c) \left(\frac{k}{k_L} \right) [F_{qn} R_{qn}^{(1)'}(c_L, \xi_s) + Q_{qn} R_{qn}^{(2)'}(c_L, \xi_s)] M_{qn}^L(c_L, c) = 0, \quad (29) \end{aligned}$$

where

$$M_{qn}^\alpha(c_\alpha, c) = \int_{-1}^1 S_{qn}(c_\alpha, \eta) S_{qn}(c, \eta) d\eta, \quad (30)$$

for $\alpha = R, L$. Writing the system of equations (24)-(29) in matrix form and the solution by matrix inversion yields the unknown coefficients associated with the scattered and transmitted fields.

III. NUMERICAL RESULTS

In the limit $\xi \rightarrow \infty$, since $c\xi \rightarrow k\rho$ with ρ being the radial cylindrical coordinate, using asymptotic expressions, the radial Mathieu function of the fourth kind and its first derivative with respect to argument can be written as:

$$\lim_{\xi \rightarrow \infty} R_{qn}^{(4)}(c, \xi) \approx j^n \sqrt{\frac{j}{k\rho}} e^{-jk\rho},$$

$$\lim_{\xi \rightarrow \infty} R_{qn}^{(4)}(c, \xi) \approx j^{n-1} k \rho \sqrt{\frac{j}{k \rho}} e^{-jk\rho}. \quad (31)$$

Using (31) and the fact that in the limit $\xi \rightarrow \infty$, $kh \rightarrow kF \cosh u \approx k\rho$, we can write expressions for the scattered electric field components in the far zone as:

$$E_z^s = \sqrt{\frac{j}{k\rho}} e^{-jk\rho} \left[\sum_{n=0}^{\infty} j^n B_{en} S_{en}(c, \cos \varphi) + \sum_{n=1}^{\infty} j^n B_{on} S_{on}(c, \cos \varphi) \right], \quad (32)$$

$$E_\varphi^s = j \sqrt{\frac{j}{k\rho}} e^{-jk\rho} \left[\sum_{n=0}^{\infty} j^n C_{en} S_{en}(c, \cos \varphi) + \sum_{n=1}^{\infty} j^n C_{on} S_{on}(c, \cos \varphi) \right], \quad (33)$$

and the scattered magnetic field components as $H_z^s = E_\varphi^s / Z$ and $H_\varphi^s = -E_z^s / Z$.

The bistatic scattering cross section is defined as:

$$\sigma = \lim_{\rho \rightarrow \infty} 2\pi\rho \frac{\text{Re}[\mathbf{E}_s \times \mathbf{H}_s^* \cdot \hat{\rho}]}{\text{Re}[\mathbf{E}_i \times \mathbf{H}_i^* \cdot \hat{\rho}]}, \quad (34)$$

with $\text{Re}[w]$ denoting the real part of the complex number w , the asterisk denoting the complex conjugate, and $\hat{\rho}$ denoting the unit vector in the increasing radial direction. Substituting for the far zone scattered fields in (34), and recalling that the incident field is of unit amplitude, an expression for the normalized bistatic width can be written as:

$$\frac{\sigma(\varphi)}{\lambda} = \left| \sum_{q=e,o} \sum_{n=0}^{\infty} j^n B_{qn} S_{qn}(c, \cos \varphi) \right|^2 + \left| \sum_{q=e,o} \sum_{n=0}^{\infty} j^n C_{qn} S_{qn}(c, \cos \varphi) \right|^2. \quad (35)$$

It can be seen from equation (35) that the uniqueness of PEMC material over PEC and PMC materials it has both co and cross-polarized field components.

Results obtained are presented graphically as normalized bistatic width for chiral coated PEMC elliptic cylinders of different sizes, PEMC admittances, and chiral coatings, with all coated cylinders assumed to be located in free space. For convenience, the PEMC admittance M is expressed in terms of the dimensionless quantity MZ_1 , using the formula $MZ_1 = \tan(\nu)$, so that $\nu=0^\circ$ and $\nu=90^\circ$ correspond to the PMC and PEC cases, respectively.

Normalized bistatic widths of chiral coated PEMC elliptic cylinders obtained for different scattering angles, when they are illuminated by a plane wave incident at 0° , are shown in Fig. 2. The geometrical parameters of the

scatterer are $a=0.4\lambda$, $b=0.2\lambda$, $a_c=0.56\lambda$, $b_c=0.44\lambda$, and the coating values are $\epsilon_{rc}=2.5$ and $\mu_{rc}=1.0$. The admittances of the PEMC cylinders are specified by the parameter ν , which varies from 0° to 90° , in steps of 15° and chiral admittance is $\zeta_c=0.0$.

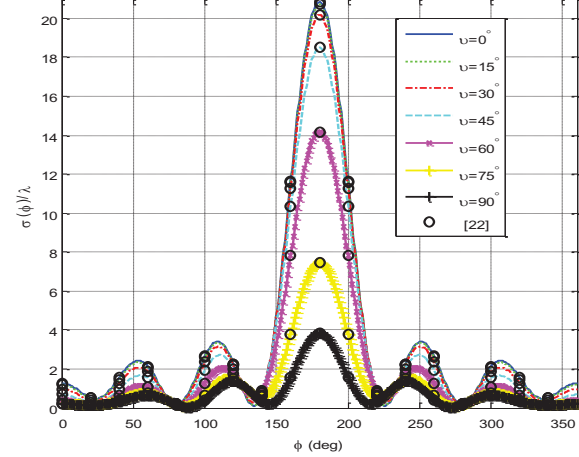


Fig. 2. Normalized bistatic width versus scattering angle for PEMC elliptic cylinders of different admittances coated with $\epsilon_{rc}=2.5$, $\mu_{rc}=1.0$, $\phi_i=0^\circ$, and $\zeta_c=0.0$.

The plots are symmetric around $\varphi=180^\circ$ as expected. The normalized bistatic width for a given scattering angle decreases as the value of ν increases, with the magnitude for each angle being a maximum for $\nu=0^\circ$ (PMC), a minimum for $\nu=90^\circ$ (PEC), and the differences for two values of ν becoming a maximum at $\varphi=180^\circ$, corresponding to forward scattering. The normalized bistatic widths are compared with the corresponding values obtained for a conventional coated PEMC elliptic cylinder in [22], presented by circles, and are in very good agreement, validating the calculations for an elliptic cylinder in general.

Figure 3 (a) is similar to Fig. 2, except that the chiral admittance is taken to be $\zeta_c=0.002$. This figure shows the effect of both PEMC and chiral coating on the bistatic of coated elliptic cylinder. There is a drop in the bistatic width by approximately of 50% at $\nu=0^\circ$ and $\nu=90^\circ$, and no change in the location of the maximum values for other values of ν . It is worth mentioning that the value of the bistatic widths for $\nu=75^\circ$ and 90° are the same at $\varphi=180^\circ$. Figure 3 (b) is similar to Fig. 3 (a), except ζ_c is reduced to 0.0015. It can be seen that the bistatic width is higher and the maximum is back at $\nu=0^\circ$ and the minimum at $\nu=90^\circ$. The variation of the bistatic widths is due to the presence of the cross-polarized fields of

PEMC and chiral materials.

Figure 4 is similar to Fig. 3, except that the incident angle is 90° . Figure 4 (a) shows that the magnitude of the bistatic width has maxima at $\nu=90^\circ$ and minima at $\nu=0^\circ$ and $\phi=90^\circ$, while the opposite is happening at the scattering angle of $\phi=270^\circ$. Figure 4 (b) is for the case of $\zeta_c=0.0015$.

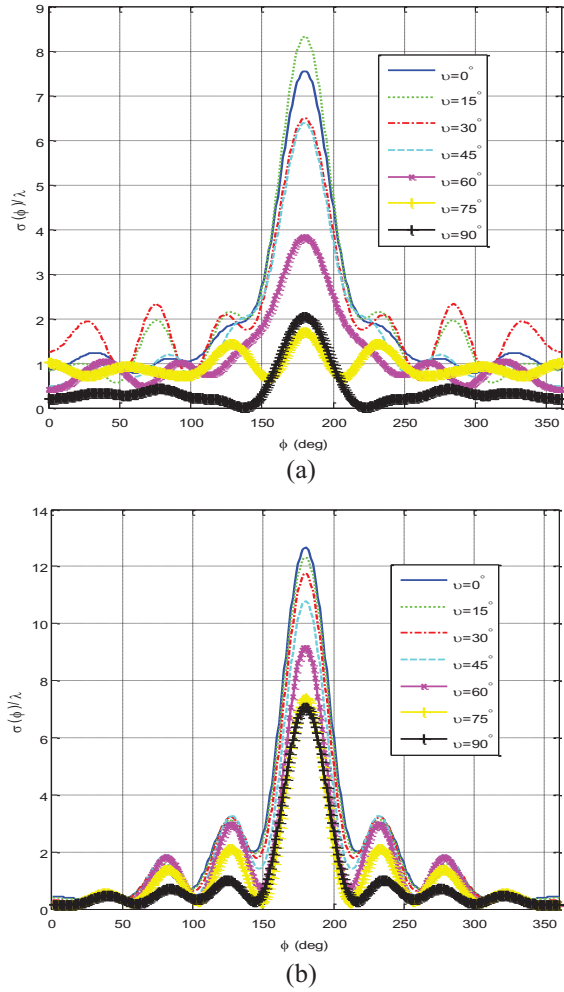


Fig. 3. Normalized bistatic width versus scattering angle for PEMC elliptic cylinders of different admittances coated with $\epsilon_{rc}=2.5$, $\mu_{rc}=1.0$, $\phi_i=0^\circ$: (a) $\zeta_c=0.002$, and (b) $\zeta_c=0.0015$.

It can be seen that Fig. 5 is similar to 4, except by increasing ϵ_{rc} from 2.5 to 3.0. Figure 6 shows the bistatic widths versus the major axis of the dielectric coating for $\nu=45^\circ$ and 75° and $\zeta_c=0.002$ and 0.0025 . The presence of chiral material effects the magnitude but not the pattern of the bistatic width. More results and analysis on chiral coated or PEMC conventional coated elliptic cylinder can be found in [22,24].

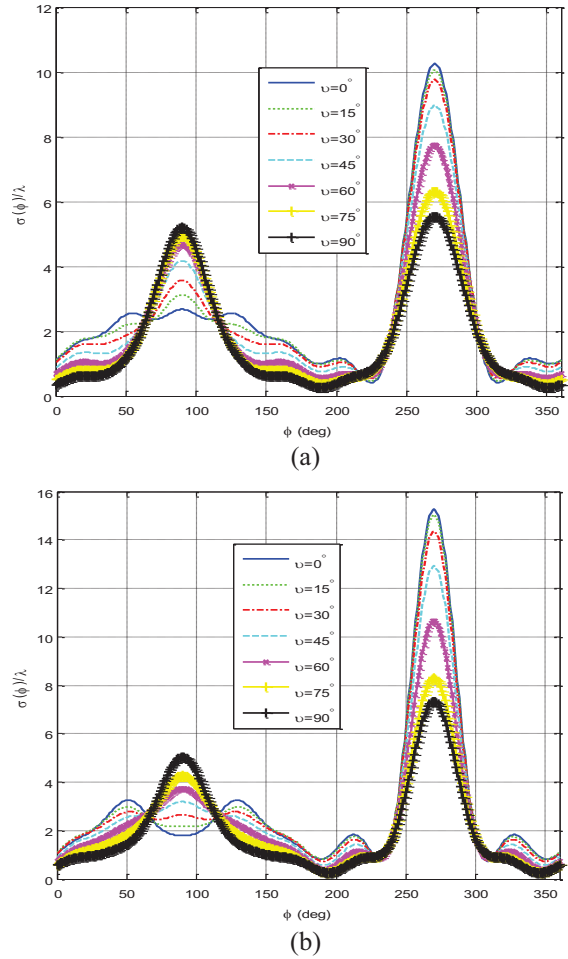


Fig. 4. Normalized bistatic width versus scattering angle for PEMC elliptic cylinders of different admittances coated with $\epsilon_{rc}=2.5$, $\mu_{rc}=1.0$, $\phi_i=90^\circ$: (a) $\zeta_c=0.002$, and (b) $\zeta_c=0.0015$.

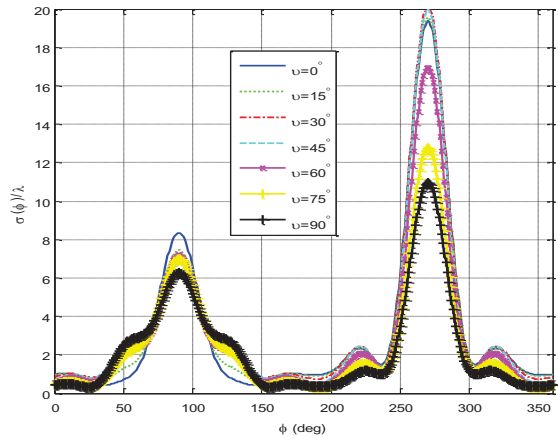


Fig. 5. Normalized bistatic width versus scattering angle for PEMC elliptic cylinders of different admittances coated with $\epsilon_{rc}=3.0$, $\mu_{rc}=1.0$, $\phi_i=90^\circ$ and $\zeta_c=0.002$.

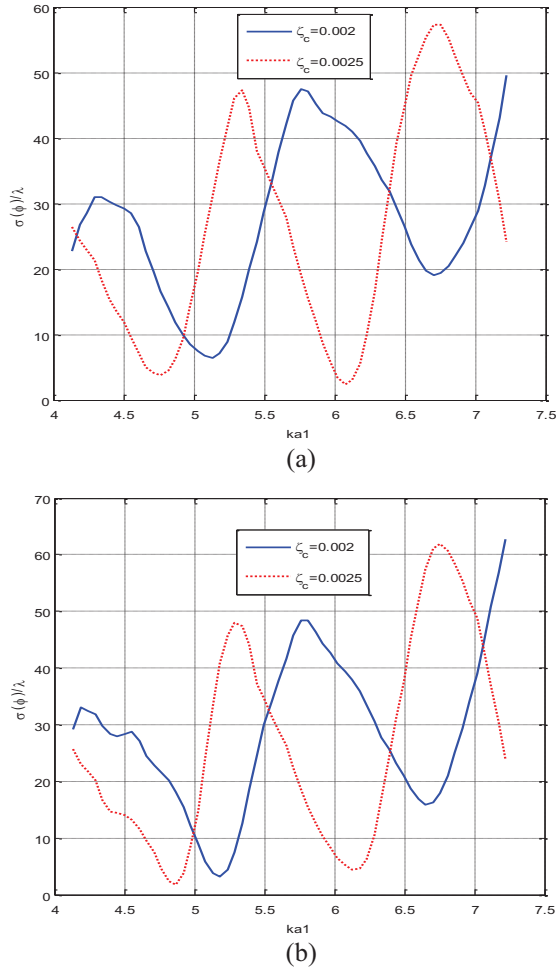


Fig. 6. Normalized bistatic width versus ka_1 for PEMC elliptic cylinders of different admittances coated with $\epsilon_{rc}=3.0$, $\mu_{rc}=1.0$, $\phi_i=0.0^\circ$, $a=0.4\lambda$, $b=0.2\lambda$: (a) $\nu=45^\circ$, and (b) $\nu=75^\circ$.

IV. CONCLUSION

Analytic solution has been obtained to the problem of scattering from a chirally coated PEMC elliptic cylinder, when it is excited by a uniform plane wave. The solution is general since it also can provide the solution to the scattering by PEMC circular or strip chiral coated geometries. The results obtained show that the admittances as well as the constitutive parameters of the chiral coating material can be used to control (enhancing or reducing) the scattering width of a coated PEMC elliptic cylinder. Thus, the solution provides the designer with two degree of freedom to control the bistatic width. The new results obtained in this paper are important, since they can be used to validate similar results obtained using other methods, and provide an insight into how the changing of various parameters associated with a chirally coated PEMC elliptic cylinder changes the scattering widths that could be obtained from it.

REFERENCES

- [1] I. V. Lindell and A. H. Sihvola, "Perfect electromagnetic conductor," *J. Electromag. Waves Appl.*, vol. 19, no. 7, pp. 861-869, 2005.
- [2] R. Ruppin, "Scattering of electromagnetic radiation by a perfect electromagnetic conductor cylinder," *J. Electromag. Waves Appl.*, vol. 20, no. 13, pp. 1853-1860, 2006.
- [3] S. Ahmed and Q. A. Naqvi, "Electromagnetic scattering from a perfect electromagnetic conductor cylinder buried in a dielectric half-space," *PIER 78*, pp. 25-38, 2008.
- [4] S. Ahmed and Q. A. Naqvi, "Electromagnetic scattering from parallel perfect electromagnetic conductor cylinders of circular cross-sections using an iterative procedure," *J. Electromag. Waves Appl.*, vol. 22, pp. 987-1003, 2008.
- [5] A. Illahi, M. Afzaal, and Q. A. Naqvi, "Scattering of dipole field by a perfect electromagnetic conductor cylinder," *PIER L 4*, pp. 43-53, 2008.
- [6] S. Ahmed and Q. A. Naqvi, "Electromagnetic scattering from a two dimensional perfect electromagnetic conductor (PEMC) rectangular strip and PEMC rectangular strip grating simulated by circular cylinders," *Optics Comm.*, vol. 281, pp. 4211-4218, 2008.
- [7] S. Ahmed and Q. A. Naqvi, "Electromagnetic scattering of two or more incident plane waves by a perfect electromagnetic conductor cylinder coated with a metamaterial," *PIER B*, vol. 10, pp. 75-90, 2008.
- [8] A. Illahi and Q. A. Naqvi, "Scattering of an arbitrarily oriented dipole field by an infinite and a finite length PEMC circular cylinder," *CEJP*, vol. 7, no. 4, pp. 829-853, 2009.
- [9] S. Ahmed and Q. A. Naqvi, "Directive EM radiation of a line source in the presence of a coated PEMC circular cylinder," *PIER 92*, pp. 91-102, 2009.
- [10] A. Sihvola, P. Ylä-Oijala, and I. V. Lindell, "Bistatic scattering from a PEMC (perfect electromagnetic conducting) sphere: surface integral equation approach," *Symp. Digest IEEE/ACES Int. Conf. Wireless Comm. Appl. Comp. Electromag.*, pp. 317-320, 2005.
- [11] R. Ruppin, "Scattering of electromagnetic radiation by a perfect electromagnetic conductor sphere," *J. Electromag. Waves Appl.*, vol. 20, no. 12, pp. 1569-1576, 2006.
- [12] A-K. Hamid and F. R. Cooray, "Scattering of electromagnetic waves by a perfect electromagnetic conducting spheroid," *IET Proc. Microwaves Antennas Propagat.*, vol. 2, no. 7, pp. 686-695, 2008.
- [13] Q. Naqvi and S. Ahmed, "Electromagnetic scattering from a perfect electromagnetic

- conductor circular cylinder coated with a metamaterial having negative permittivity and/or permeability,” *Optics Comm.*, vol. 281, pp. 5664-5670, 2008.
- [14] R. Ruppın, “Scattering of electromagnetic radiation by a coated perfect electromagnetic conductor sphere,” *PIER L*, vol. 8, pp. 53-62, 2009.
- [15] I. V. Lindell and A. H. Sihvola, “Perfect electromagnetic conductor,” *J. Electromag. Waves Appl.*, vol. 19, no. 7, pp. 861-869, 2005.
- [16] A. Sihvola, I. V. Lindell, and P. Ylä-Oijala, “Scattering properties of PEMC (perfect electromagnetic conducting) materials,” *Symp. Digest PIERS*, Hangzhou, China, Aug. 2005.
- [17] I. V. Lindell and A. H. Sihvola, “Perfect electromagnetic conductor (PEMC) in electromagnetics,” *Symp. Digest PIERS*, Hangzhou, China, Aug. 2005.
- [18] I. V. Lindell and A. H. Sihvola, “Transformation method for problems involving perfect electromagnetic conductor (PEMC) structures,” *IEEE Trans. Antennas Propag.*, vol. 53, no. 9, pp. 3005-3011, 2005.
- [19] H. A. Ragheb and L. Shafai, “Electromagnetic scattering from a dielectric-coated elliptic cylinder,” *Can. J. Phys.*, vol. 66, no. 12, pp. 1115-1122, 1988.
- [20] S. Ahmed, F. Manan, A. Shahzad, and Q. A. Naqvi, “Electromagnetic scattering from a chiral-coated PEMC cylinder,” *Progress In Electromagnetics Research M*, vol. 19, pp. 239-250, 2011.
- [21] M. Khalid, A. A. Syed, and Q. A. Naqvi, “Circular cylinder with D’B, DB’ and D’B’ boundary conditions placed in chiral and chiral nihility media,” *International Journal of Applied Electromagnetics and Mechanics*, vol. 44, pp. 59-68, 2014.
- [22] F. Cooray and A-K. Hamid, “Scattering from a coated perfect electromagnetic conducting elliptic cylinder,” *International Journal of Electronics and Communications, AEUE*, vol. 66, pp. 472-479, 2012.
- [23] P. M. Morse and H. Feshbach, *Methods of Theoretical Physics, Part II*, McGraw Hill, New York, 1953.
- [24] A-K. Hamid and F. Cooray, “Scattering from a chirally coated DB elliptic cylinder,” *International Journal of Electronics and Communications, AEUE*, vol. 68, pp. 1106-1111, 2014.



A-K. Hamid received the B.Sc. degree in Electrical Engineering from West Virginia Institute of Technology and University, West Virginia, U.S.A. in 1985, the M.Sc. and Ph.D. degrees from the University of Manitoba, Winnipeg, Manitoba, Canada in 1988 and 1991, respectively, both in Electrical Engineering. From 1991-1993, he was with Quantic Laboratories Inc., Winnipeg, Manitoba, Canada, developing two and three dimensional electromagnetic field solvers using boundary integral method. From 1994-2000 he was with the Faculty of Electrical Engineering at King Fahd University of Petroleum and Minerals, Dhahran, Saudi Arabia. Since Sept. 2000, he has been with the Electrical and Computer Engineering Department at the University of Sharjah, Sharjah, United Arab Emirates. His research interest includes EM wave scattering from two and three dimensional bodies, propagation along waveguides with discontinuities, FDTD simulation of cellular phones, and inverse scattering using neural networks.